Plasticity at the micron scale

John W. Hutchinson*

Division of Engineering and Applied Sciences, Harvard University, Cambridge MA 02138, USA

Abstract

Over a scale which extends from about a fraction of a micron to tens of microns, metals display a strong size-dependence when deformed non uniformly into the plastic range: smaller is stronger. This effect has important implications for an increasing number of applications in electronics, structural materials and MEMS. Plastic behavior at this scale cannot be characterized by conventional plasticity theories because they incorporate no material length scale and predict no size effect. While micron sized solid objects are too small to be characterized by conventional theory, they are usually too large to be amenable to analysis using approaches presently available based on discrete dislocation mechanics. The relatively large numbers of dislocations governing plastic deformation at the micron scale motivate the development of a continuum theory of plasticity incorporating size-dependence. Strain gradient theories of plasticity have been developed for this purpose. The motivation and potential for such theories will be discussed. Important open issues surrounding the foundations of strain gradient plasticity will also be addressed and a few critical experiments identified. © 1999 Elsevier Science Ltd. All rights reserved.

1. Size-dependence at the micron scale

Applications of metals and polymers at the micron scale are multiplying rapidly. Plasticity as well as the elasticity of the materials are important in many of these applications, and efforts are underway in the materials and mechanics communities to measure and characterize behavior at the micron scale.

Indentation tests are a common means of assessing material yield strength. Instruments have been developed which permit measurement of indentation hardness at the micron and nano scales. A large size-dependence is observed in indentation tests on metals. Data for tungsten single crystals at three orientations relative to the indenter are shown in Fig. 1. The hardness is defined as the indentation load divided by the area of the indent after unloading. The Vickers indenter is relatively shallow so that the indentation depth is a fraction of the indentation diagonal plotted in Fig. 1. There is some dependence

---

* Tel: +1-617-495-2848; Fax: +1-617-495-9837.
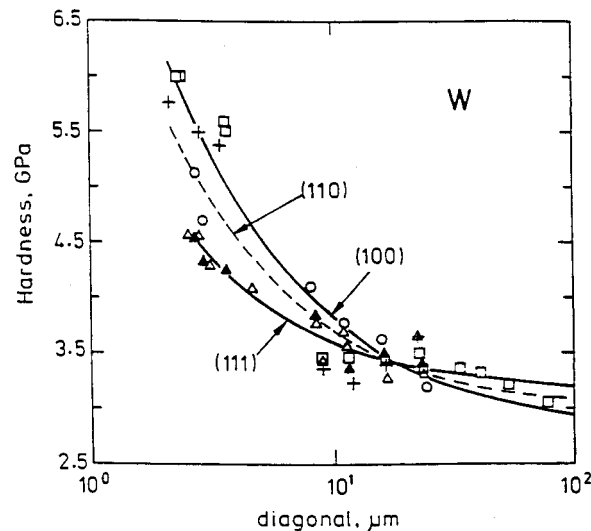 *E-mail address:* hutchinson@husm.harvard.edu (J.W. Hutchinson)

Fig. 1. Hardness data for tungsten single crystals at three orientations relative to the Vickers indenter (Stelmashenso et al., 1993). The hardness (load divided by the area of the indent) is plotted against the diagonal of the four-sided pyramidal indent displaying the increase in hardness with decrease in indent size.

of hardness on crystal orientation, but the size-dependence is the predominant effect. Indents with diagonals longer than about 100μm cease to display any size-dependence. By simple dimensional arguments, it follows that any conventional plasticity theory (e.g. one that does not possess a constitutive length scale) necessarily implies indentation hardness would be size-independent. The strong size-dependence evident at the micron scale in Fig. 1 and in data on other metals (Atkinson, 1995, Ma and Clarke, 1995; De Guzman et al., 1993; McElhaney et al., 1998; Poole et al., 1996) constitutes one of the compelling pieces of experimental evidence for the need of an extension of plasticity theory to the micron scale. Here and throughout this paper, the term 'micron scale' will be used to refer to the range which extends roughly from a fraction of a micron to tens of microns. At even smaller scales, dislocation mechanics is required to understand nucleation of dislocations at the indenter and the interaction between relatively small numbers of individual dislocations. Recent modeling efforts of nano scale indentation of single crystals based on discrete dislocation mechanics appear promising (Tadmore et al., 1998). At the micron scale, the number of dislocations involved in the indentation zone is usually large — too large to be amenable at the present time to quantitative analysis using dislocation mechanics.

A second set of experiments displaying strong size-dependence of plastic deformation in the micron range is displayed in Fig. 2. Annealed copper wires of diameter ranging from 170 down to 12μm are twisted well into the plastic range. For each wire, the torque, Q, versus twist per unit length, κ, is plotted as Q/a^3 versus κa, where a is the radius of the wire (Fig. 2a). Dimensional arguments dictate that, had the wires been governed by a continuum theory with no constitutive length parameter, the curves of Fig. 2a should plot on top of one another. The factor of three strength advantage of the smaller wires over the largest wire reflects the size effect. Tensile stress–strain data for these same wire are plotted in Fig. 2b. These do superimpose, to within experimental error. The strengthening effect at the micron scale is intrinsically associated with non-uniform deformation, as will be discussed shortly.

Test data for plastic bending of a series of 'micron' thick nickel films is presented in Fig. 3. Strips of the film were bent around a series of fibers of different diameters. Elastic springback upon release of the
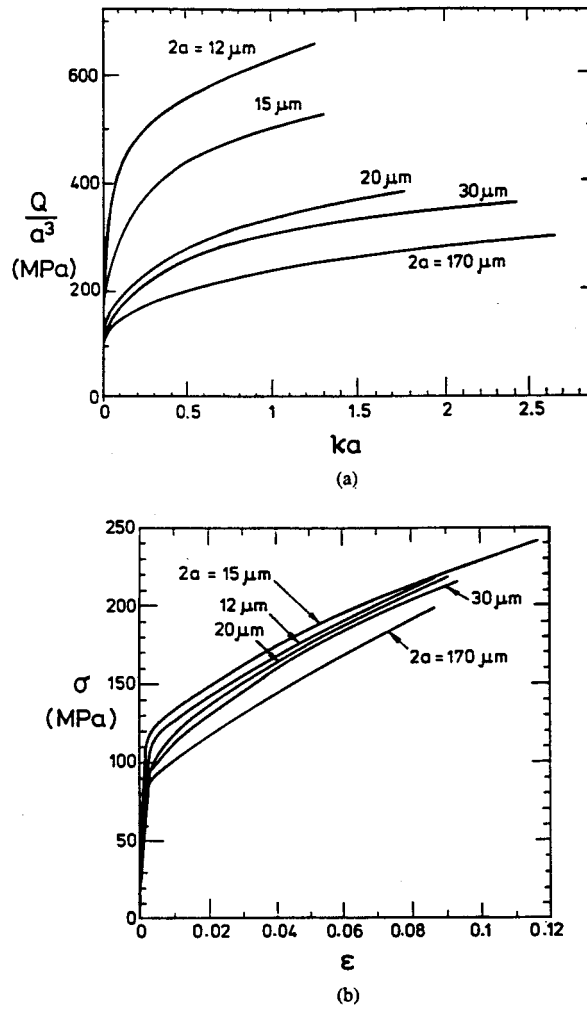
Fig. 2. Data for torsion and tension of fine polycrystalline copper wires (Fleck et al., 1994). (a) Torque versus twist per unit length normalized in such a way that the curves for a material with no internal constitutive length scales must fall on top of one another. The plot brings out the increased effective strength of the smaller wires in torsion. (b) Uniaxial stress versus strain. There is essentially no size-effect in uniaxial tension.

film was measured providing the moment M associated with the curvature of the fiber κ. The bending data in Fig. 3 is plotted as M/bh^2 versus the surface strain, $\varepsilon_b = \kappa h/2$, where h is the film thickness and b is the strip width. As in the case of wire torsion, the bending data presented this way should be independent of film thickness were no material length parameters operative. The large apparent strengthening of the thinner films over the thicker ones is similar to that observed for the wires in torsion. The tensile data shows some size-dependence with thinner films having *smaller* strength than thicker ones, an effect attributed to the grain structures of the films. A rescaling of the data in Fig. 3 to account for this grain effect further amplifies the trend of increasing strength with decreasing film thickness (Stölken and Evans, 1998).

The size-dependence yield strength displayed in each of the three examples is believed to be associated
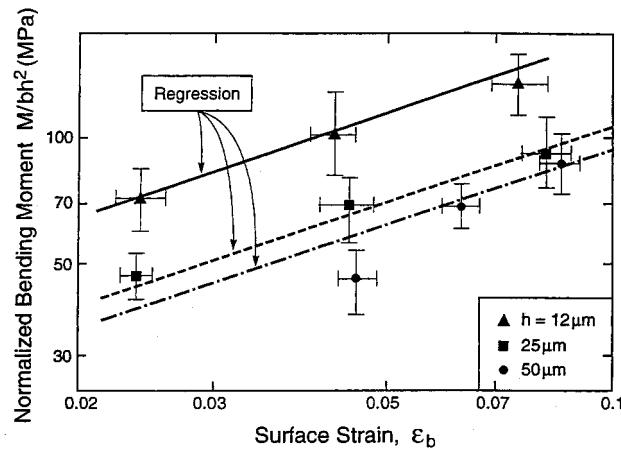
Fig. 3. Normalized bending moment versus normalized curvature ($\varepsilon_b = \kappa_h/2$) for initially straight thin films of nickel subject to bending (Stölken and Evans, 1998). The data is presented in such a way that responses for materials with no internal constitutive length scale would superimpose. In this way, the figure brings out the strength increase of thinner films relative to thicker films in bending.

with geometrically necessary dislocations generated by non-uniform straining (Ashby, 1970; Fleck et al., 1994; Nix and Gao, 1998). An elementary argument is outlined in the next two paragraphs.

In principle, uniform straining of a pure crystal could occur without any dislocations being stored. However, dislocations do accumulate due to statistical interaction with one another and with the microstructural features such as precipitates leading to statistically stored dislocations whose density, ρ_s, increases with strain in a complex manner. By contrast, plastic deformation associated with a strain gradient imposed on the crystal in most instances (but not all) requires a definite density of dislocations ρ_G to be present, the so called geometrically necessary dislocations. The density of geometrically necessary dislocations is directly proportional to the gradient of plastic strain. In the simplest view, the total dislocation density at a point in the deformation history is the sum of the statistically stored and geometrically necessary dislocations. The flow stress depends on these two contributions in accord with Taylor's relation $\tau_Y = c\mu b\sqrt{\rho_s + \rho_G}$, where c is a number which depends on crystal type, μ is the elastic shear modulus and b is the magnitude of Burger's vector.

Consider a material element subject to an increment of plastic stain $\dot{\varepsilon}^p$ and strain gradient $\partial\dot{\varepsilon}^p/\partial x$ with associated increments of dislocation densities $\dot{\rho}_s$ and $\dot{\rho}_G$. For purposes of discussion, suppose that plastic strain increments are entirely associated with the generation of new dislocations. With L as the average distance a newly generated dislocation travels, $\dot{\varepsilon}^p \propto \dot{\rho}_s bL$. Geometrically necessary dislocations accumulate in proportion to the strain gradient such that $\partial\dot{\varepsilon}^p/\partial x \propto \dot{\rho}_G b$. If follows that $\dot{\rho}_G < \dot{\rho}_s$ if $(\partial\dot{\varepsilon}^p/\partial x)L < \dot{\varepsilon}^p$, while increments of the two dislocation densities become comparable $\dot{\rho}G \approx \dot{\rho}_S$ if $(\partial\dot{\varepsilon}^p/\partial x)L \approx \dot{\varepsilon}^p$. Thus, L is the length scale at which plastic strain gradients significantly influence flow stress increments via Taylor's relation. A derivation of the length scale using alternative assumptions has been given by Nix and Gao (1998) leading to $b(\mu/\sigma_0)^2$, where σ_0 is a reference flow stress in the absence of a strain gradient. In either case, the length scale characterizing strain gradient plasticity is very large compared to the atomic lattice spacing. A phenomenological theory will be discussed in the next section which requires constitutive length parameters in the range from 1/4 to 5 μm to fit the experimental data of Figs. 1–3.

The step of translating from the simple dislocation equations to a continuum formulation is not obvious. Statistically stored dislocations are imagined to be dependent on the plastic strains ε^p, while

geometrically necessary dislocations are dependent on strain gradients $\partial \varepsilon^p / \partial x$. In a continuum theory, these two contributions can be combined in various ways for which there is little guidance from dislocation mechanics. Two proposals will be mentioned to illustrate the leeway. Fleck et al. (1994) imagine that the dislocation density increases in proportion to the measure $((\varepsilon^p)^\lambda + (\ell \partial \varepsilon^p / \partial x)^\lambda)^{1/\lambda}$ where ℓ is the new constitutive length scale and values of λ between 1 and 2 have been considered. Guided by the Taylor relation, the flow stress is taken to be a function of this measure. The choice $\lambda = 2$ used in most of the subsequent studies based on this formulation has been made for mathematical reasons, not physical ones. Nix and Gao (1998), followed by Gao et al. (1998), use the flow stress in the absence of strain gradients as their starting point. If this flow stress depends on plastic strain in proportion to $f(\varepsilon^p)$, it follows from the Taylor relation that the density of statistically stored dislocations in the absence of strain gradients is proportional to $f(\varepsilon^p)^2$. Strain gradients are incorporated into the higher order theory by taking the flow stress dependence to be $\sqrt{f(\varepsilon^p)^2 + \ell \partial \varepsilon^p / \partial x}$. This choice is tantamount to assuming the geometrically necessary dislocations have no direct influence on the accumulation of the statistically stored dislocations. The implications of this combination of the plastic strains and strain gradient for the formulation of a strain gradient theory are discussed by Gao et al. (1999).

2. Phenomenological theory of strain gradient plasticity: applications at the micron scale

2.1. Sketch of the theory and constitutive length parameters

Several phenomenological plasticity theories have been proposed which incorporate a dependence on plastic stain gradients Aifantis (1984, 1992), Acharya and Bassani (1996), de Borst and Muhlhaus (1992), Fleck et al. (1994), Gao et al. (1999), and discussion focusing on the differences among some of them will be given in Section 3. The most fundamental theories focus on single crystal deformation, and derive relationships of plastic strains and strain gradients to slips and slip gradients. In this section, the generalization due to Fleck and Hutchinson (1997) of the most widely used conventional theory, J_2 flow theory, to include strain gradients will be used as the basis for discussion. This is an phenomenological theory. At this point in the development of the subject this particular version of the theory is the most highly developed, and its implications for a variety of applications have been most extensively explored. The theory will be designated in short by J_2 SGP theory. The reader is referred to the article by Fleck and Hutchinson (1997) for full details of the theory. Here, only those elements of the theory necessary to discuss the implications of the theory will be given. As in the case of conventional J_2 theory, the strain gradient version has both a deformation version (a small strain, nonlinear elasticity intended for nominally proportional loading histories) and an incremental version with a yield surface and provision for loading and unloading. Deformation theory will be adequate to illustrate the essential points for this overview of phenomena and applications.

The deformation theory version of J_2 SGP theory makes of an effective strain measure defined by

$$E_e^2 = \frac{2}{3}\varepsilon_{ij}{}'\varepsilon_{ij}{}' + \ell_1^2 \eta_{ijk}{}'^{(1)}\eta_{ijk}{}'^{(1)} + \ell_2^2 \eta_{ijk}{}'^{(2)}\eta_{ijk}{}'^{(2)} + \ell_3^2 \eta_{ijk}{}'^{(3)}\eta_{ijk}{}'^{(3)} \tag{1}$$

where ε_{ij} is the strain, $\varepsilon_{ij}{}'$ is the deviatoric strain, $\eta_{ijk} = u_{k,ij}$ is the strain gradient and $\eta_{ijk}{}'$ is its deviator. The three strain gradient quantities, $\eta_{ijk}{}'^{(I)}$, have the property that they are mutually orthogonal $\eta_{ijk}{}'^{(I)}\eta_{ijk}{}'^{(J)} = 0, I \neq J$). Any strain gradient deviator $\eta_{ijk}{}'$ can be uniquely represented as a sum of these three tensors (Smyshlyaev and Fleck, 1996). The effective strain measure is the most general isotropic combination of quadratic terms in the strain deviator and strain gradient deviator. Deformation theory postulates an energy density, $W(E_e, \varepsilon_{kk})$, chosen to reproduce data for a monotonic uniaxial (or shear)

stress history and to have elastic compressibility. The stress and higher order stress are generated from

$$\sigma_{ij} = \frac{\partial W}{\partial \varepsilon_{ij}}, \tau_{ijk} = \frac{\partial W}{\partial \eta_{ijk}} \tag{2}$$

The deformation version falls with the class of solids considered by Toupin (1962) and Mindlin (1965). The virtual work statement of equilibrium is

$$\int_V [\sigma_{ij}\delta\varepsilon_{ij} + \tau_{ijk}\delta\eta_{ijk}]dV = \int_A [t_i\delta u_i + r_i n_j \delta u_{i,j}]dA \tag{3}$$

where η_i is the outward unit normal to the surface, $r_i = n_j n_k \tau_{jki}$ is the double stress acting on the surface, and the surface traction is

$$t_k = n_i(\sigma_{ik} - \tau_{ijk,j}) + n_i n_j \tau_{ijk}(D_p n_p) - D_j(n_i \tau_{ijk}) \tag{4}$$

with the surface gradient being $D_j = (\delta_{jk} - n_j n_k)\partial_k$.

Important insight into the origin of strain gradient contributions comes from the observation that the second and third invariants of the strain gradient in Eq. (1) depend only on the rotation gradient $\chi_{ij} = \theta_{i,j} = e_{ipk}\varepsilon_{kj,p}'$ where the rotation is $\theta_i = e_{ijk}u_{k,j}/2$. The equivalent strain can be rewritten as

$$E_e^2 = \frac{2}{3}\varepsilon_{ij}'\varepsilon_{ij}' + \ell_1^2 \eta_{ijk}'^{(1)}\eta_{ijk}'^{(1)} + \frac{2}{3}\left(2\ell_2^2 + \frac{12}{5}\ell_3^2\right)\chi_{ij}\chi_{ij} + \frac{2}{3}\left(2\ell_2^2 - \frac{12}{5}\ell_3^2\right)\chi_{ij}\chi_{ji} \tag{5}$$

Solutions to a fairly wide group of problems suggests that the last term in the effective strain depending on $\chi_{ij}\chi_{ji}$ plays an unessential role in most problems. To reduce the set of new constitutive length parameters from three to two, the term depending on $\chi_{ij}\chi_{ji}$ is omitted from consideration in the sequel and the effective strain is taken to be

$$E_e^2 = \frac{2}{3}\varepsilon_{ij}'\varepsilon_{ij}' + \ell_{SG}^2 \eta_{ijk}'^{(1)} + \frac{2}{3}\ell_{RG}^2 \chi_{ij}\chi_{ij} \tag{6}$$

The notation for the two constitutive length parameters reflects the fact that $\eta_{ijk}'^{(1)}\eta_{ijk}'^{(1)}$ depends on stretch gradients (and rotation gradients), while $\chi_{ij}\chi_{ij}$ depends only on rotation gradients. If dependence on stretch gradients is eliminated ($\ell_{SG} = 0$), the theory reduces to that for a couple stress solid (Fleck and Hutchinson, 1994). When stretch gradients are included the full Toupin-Mindlin framework applies.

There has already been some progress in identifying the constitutive length parameters for a few materials, although these efforts must still be regarded as preliminary at this stage in the development of the subject. Wire torsion depends only on ℓ_{RG} (or ℓ_2). The best fit of the strain gradient theory to the experimental data for the annealed copper wires in Fig. 2 gives $\ell_{RG} \cong 4\,\mu m$ (Fleck et al., 1994). A fit of theory to the bending tests on nickel films of Fig. 3 gives $\sqrt{\ell_{RG}^2 + \frac{8}{5}\ell_{SG}^2} \cong 5\mu m$ (Stölken and Evans, 1998). Numerical calculations modeling indentation based on the theory have been performed (Begley and Hutchinson, 1998). While rotation gradients are not zero in indentation, they are much less important than stretch gradients, and the size-dependent hardness trends seen in Fig. 1 are predicted by the theory to be primarily tied to ℓ_{SG}. Fit of the theory to indentation data such as that of Fig. 1, for a number of metals gives ℓ_{SG} in the range from as small as 0.25 μm to about 1 μm. If this range of values is accepted, one sees that film bending is dominated by the rotation gradient, and the finding for the nickel film becomes $\ell_{RG} \cong 5$ μm, which is not very different for the determination for the copper. Thus, based on the experimental data available at the present time, it appears that there is not a large variation in the constitutive length parameters from metal to metal and tentatively we conclude

$$\ell_{SG} \approx 0.25 \text{ to } 1\mu m \quad \ell_{RG} \approx 5\mu m \qquad (7)$$

The indentation study brought out some dependence on hardening level, with the hardest materials having the smaller length parameter. In the discussion of examples which follows, the values identified in Eq. (7) will be taken as representative.

2.2. Applications and implications of strain gradient plasticity

Size effects in plasticity are well known in other contexts than indentation, wire torsion and film bending. The Hall–Petch grain size dependence of polycrystals is one of the best known examples. The flow stress of a ceramic particle-reinforced metal matrix composite is observed to increase with decreasing particle size for particles in the micron size range, all other factors such as particle volume fraction being held constant. There is no length scale in conventional plasticity to set the width of shear bands, yet they often have widths measured in microns. The implications of J_2 SGP theory for several phenomena will be discussed. As long as the length scale of the deformation field is long compared to the constitute length parameters there will be no size effect because the theory reduces to the conventional J_2 theory in this limit. The theory is intended for applications where the problem size scale is in the micron range. As illustrated earlier, the size can range from a fraction of a micron to tens of microns, depending on the problem. In addition to the applications mentioned above, the theory has important implications for void growth, thin films and crack growth. It is also likely that, as metals are used to replace silicon in the fabrication of micron electro-mechanical devices (MEMS), applications of strain gradient plasticity will arise in this area. The applications which follow are discussed using results based on J_2 SGP theory. They should be regarded as illustrative of what can be obtained from any SGP theory.

Bonded ceramic particles in a metal matrix induce gradients in plastic strain in the vicinity of the particle when the composite is subject to overall plastic strain. The gradients require geometrically necessary dislocations to be generated (Ashby, 1970) producing extra hardening of the matrix in the vicinity of the particle. For spherical particles of radius a, the effect, which depends on ℓ/a (Fleck and Hutchinson, 1997), results in greater strengthening due to smaller particles than large ones if all other details of the particle distribution are the same. Particles induce both stretch and rotation gradients in the matrix, thus the effect depends on the particular combination of ℓ_{SG} and ℓ_{RG}. Given the values in Eq. (7), calculations indicate the strength of a composite with 5 micron diameter particles will be approximately double that of one with particles at least several times that size. This is the range that size effects in particle strengthening have been observed (Lloyd, 1994). The shell of gradient hardened matrix around the particle creates an effectively larger particle. That is, it is as if the radius of the particle were larger by an amount proportional to the constitutive length parameter. There is also some influence of the specific boundary condition assumed at the particle-matrix interface. These effects arise because J_2 SGP theory is a higher order theory and additional conditions other than continuity of displacements and tractions must be specified at the interface. Discussion of these effects are taken up in Section 3. Two dimensional simulations of particle reinforcement of a metal matrix composite based on dislocation mechanics have revealed the accumulation of geometrically necessary dislocations and the particle size effect (Cleveringa et al., 1997). Simulations of this type can be used to explore open issues surrounding continuum strain gradient plasticity theories, including the question discussed in the next section as to whether higher order theories are required.

The implications of J_2 SGP theory for *void growth in a solid undergoing plastic straining* are interesting and potentially important to the understanding of ductile fracture. Void growth involves nearly irrotational deformations and, consequently, only the stretch gradient length parameter ℓ_{SG} has any significant influence. Plastic stain gradients in the vicinity of the void produce extra hardening that
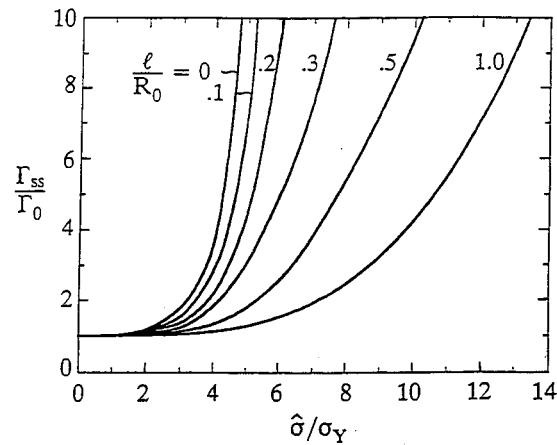
Fig. 4. Effect of strain gradient hardening on crack growth. Strain gradient hardening enables the peak separation stress to be obtained at lower overall applied loads thereby reducing the total work of fracture. The figure shows the ratio of the total steady-state work of fracture to the work of separation of the fracture process, Γ_{ss}/Γ_o, as a function of the ratio of the peak separation stress to the tensile yield stress, $\hat{\sigma}/\sigma_y$, for various values of the dimensionless constitutive length scale ℓ/R_0. The computations are based on a model which embeds the traction-separation behavior of the fracture process within the continuum J_2 SGP material (Wei and Hutchinson, 1997). The limit for $\ell/R_0=0$ is that for conventional J_2 flow theory. The calculations have been carried out for a material with a strain hardening index $N = 0.2$ and $\ell \equiv \ell_{SG} = \ell_{RG}$.

makes it more difficult for the void to grow. The effect begins to become significant when $\ell_{SG}/a \cong 1/2$ (Fleck and Hutchinson, 1997). For $\ell_{SG}=0.5$ μm, for example, voids with diameters larger than about 2 μm will be relatively unaffected, but smaller voids should begin to display a size effect. The smaller the void, the more resistant it will be to growth. Or, in the case of cavitation, the smaller the void, the higher the stress need to produce cavitation. Issues related to the appropriate higher order boundary at the free surface of the void will have some effect on this finding yet to be explored. Nevertheless, a clear warning emerges from the strain gradient plasticity theory. *Application of void growth prediction based on the conventional plasticity to submicron sized voids is probably unjustified.* The widespread use of models such as the Gurson model, which is derived from conventional plasticity, in ductile fracture applications has been for the most part limited to fracture processes with voids that are micron-size or larger. Without some modification, application of the Gurson model to processes involving submicron-size voids would appear to be questionable.

Crack tips and strain gradients go hand-in-hand. *The elevation in stress due to plastic strain gradients observed in indentation, bending and torsion are expected to have a profound effect on fracture models when the size of the fracture process zone is sub-micron.* Macroscopic loads communicated to the level of atomic or molecular separation will almost certainly be influenced by a surrounding zone of gradient hardening (Evans et al., 1998). On the other hand the so-called ductile fracture processes based on void growth and coalescence occur on a scale of tens of microns or more, and conventional plasticity should serve adequately in models to link macroscopic behavior to the fracture process. Studies of crack tip fields using strain gradient plasticity (Xia and Hutchinson, 1996; Huang et al., 1997; Wei and Hutchinson, 1997) reveal that rotation gradients play a relatively small role in altering the stresses at the crack tip in mode I, not unlike the situation for indentation. Stretch gradients, however, do have a major effect on the traction ahead of a mode I crack tip. The controlling nondimensional parameter is ℓ_{SR}/R_0. Here R_0 is a fundamental length quantity that scales the plastic zone size defined by

$$R_0 = \frac{1}{3\pi(1-v^2)} \frac{E\Gamma_0}{\sigma_Y^2} \qquad (8)$$

where σ_Y is the tensile yield stress, E and v are Young's modulus and Poisson's ratio, and Γ_0 is the work of separation of the fracture process. The effect of strain gradient hardening on the ratio of the macroscopic steady-state work of fracture to the work of the fracture process as predicted by J_2 SGP theory is shown in Fig. 4. The curve labeled $\ell_{SR}/R_0 = 0$ is the prediction for conventional J_2 theory. Under steady-state, small scale yielding conditions, the total work of fracture Γ_{ss} is the sum of Γ_0 and the dissipation occurring in the plastic zone surrounding the fracture process. Gradient hardening enables the peak separation stress $\hat{\sigma}$ to be obtained at a lower level of remote (macroscopic) load thereby shrinking the plastic zone and lowering the plastic dissipation contribution.

Thin films are ubiquitous in modern technology. Plasticity in very thin metal films, particularly those grown epitaxially, with thicknesses less than about a hundred nanometers lie outside the scope of continuum theory. 'Thick' films with thicknesses in the micron range are candidates for strain gradient plasticity. The effect of strain gradient hardening on shear lag at the edge of a highly stressed film bonded to a substrate is readily appreciated. When the film stress σ is large enough to cause yielding in shear at the film/substrate interface near the film edge, the length of the yield zone is proportional to $(\sigma/\tau_y)t$ where τ_Y is a measure of the shear yield stress of the film and t is its thickness. Strain gradient hardening will result in an increase in the effective flow stress τ_Y, increasing the shear stress on the interface and decreasing the length of the zone of plastic yielding. Rotation gradients are dominant in the shear lag zone, and this suggests that the effects should already be prominent for fairly thick films because $\ell_{RG} \cong 5\,\mu m$. There are significant consequences for the through-thickness distribution of plastic strain in the interior of the film related to conditions at the interface and free surface that can be modeled by the higher order strain gradient theory. These are discussed in the next section.

3. Is a higher order theory necessary?

Incorporation of a constitutive dependence on strain gradients raises a number of fundamental issues not the least of which is the necessity of introducing a theory such as J_2 SGP theory having higher order stresses and extra boundary conditions. Acharya and Bassani (1996), followed by Dai and Parks (1998), proposed a version of strain gradient theory which retains the lower order formulation. These authors adopt the conventional equilibrium equations and boundary conditions but take the incremental tangent moduli to be functions of the strains and strain gradients:

$$\dot{\sigma}_{ij} = L_{ijkl}(\varepsilon,\eta)\dot{\varepsilon}_{kl} \qquad (9)$$

The obvious appeal of this formulation is that it remains within the framework of classical 'lower order' incremental plasticity for which robust numerical methods have been available for many years. Higher order stresses do not appear in these theories. This approach has not been developed nor explored to the same extent as J_2 SGP theory, and it still remains to be seen if this theory can adequately reproduce observed size-effects such as those displayed in Figs. 1–3. A more fundamental issue is whether higher order stresses and boundary conditions *should* be brought into the picture along with strain gradients. The theory of elastic composites gives a clue to this issue. Moreover, there are important physical consequences that follow form a higher order theory concerning plastic deformation at free surfaces and interfaces which are absent in lower order theories. Several of these will be discussed, along with suggestions for experiments which might help to clarify the basic issue.

First consider a two-phase composite comprised of spheres of one conventional linear elastic solid distributed within and bonded to a matrix of another conventional linear elastic solid. When the

wavelength of the overall deformation is very long compared to the spacing of the spheres, standard composite theory can be used to determine the elastic energy density function in terms of the macroscopic strain and the elastic properties and spatial distribution of two phases. However, when the wavelength of overall deformation begins to become comparable to the average spacing of the spherical phase, one can determine the effect of both the macroscopic strain gradients and strains on the elastic energy density (Drugan and Willis, 1996). An approach along these lines might be followed if one desired to develop an improvement on standard composite theory for applications where the macroscopic deformation wavelengths begin to become comparable to the spacing of the spheres. A energy density depending on macroscopic strains and strain gradients will involve the spacing between the spheres as a constitutive parameter. An elasticity theory based on this energy density necessarily involves higher order stresses, which are the stress-like quantities conjugate to the strain gradients via Eq. (2). In this sense, higher order stresses are no more esoteric than strain gradients: one implies the other, even though the composite is comprised of conventional elastic phases.

It is reasonable to assume that the above line of argument carries over to elastic-plastic solids. Although the basis of dislocation mechanics is conventional elasticity theory, dislocation nucleation and interaction are so complicated that reliance on continuum plasticity is commonplace, except when relatively few dislocations are involved. If overall deformation wavelengths are such as to force consideration of strain gradients in continuum theories to account for the storage of geometrically necessary dislocation, why should higher order stresses not come into play in these theories? Intuition in interpreting higher order stresses is not well developed within the continuum mechanics community but this does not constitute a valid argument against higher order theory.

Additional boundary and interface conditions arise in a higher order theory. These can have important implications in specific applications which have yet to be subject to experimental verification. Thought experiments such as that mentioned below for thin films are suggestive, but the real test for whether a higher order strain gradient theory is required will rest on the outcome of some well chosen experiments. Dislocation models such as those used to explore particle strengthening by Cleveringa et al. (1997) should also be useful tools for this purpose.

As an example, consider boundary condition possibilities at a planar surface or interface perpendicular to the x_3 coordinate axis. Boundary conditions which follow from the virtual work statement Eq. (3) involve combinations of the following traction displacement pairs

$$t_k \text{ or } u_k$$

$$r_k \text{ or } u_{k,3} \tag{10}$$

where

$$t_k = \sigma_{3k} - 2\tau_{3jk,j} + \tau_{33k,3}$$

$$r_k = \tau_{33k} \tag{11}$$

Conditions of no constraint on displacements or displacement gradients at a free surface would require $t_k = 0$ and $r_k = 0$. Full constraint conditions at an interface where a deformable material is bonded to a rigid substrate can be enforced as $u_k = 0$ and $u_{k,3} = 0$. In conventional theory only the first of these respective pairs could be enforced. Consider the implications for a metal film in the micron thickness range bonded to a ceramic substrate and deformed by, for example, thermal expansion mismatch between the film and the substrate. Well away from the edges of the film/substrate system, conventional theory predicts that the film deforms uniformly through the thickness. The boundary
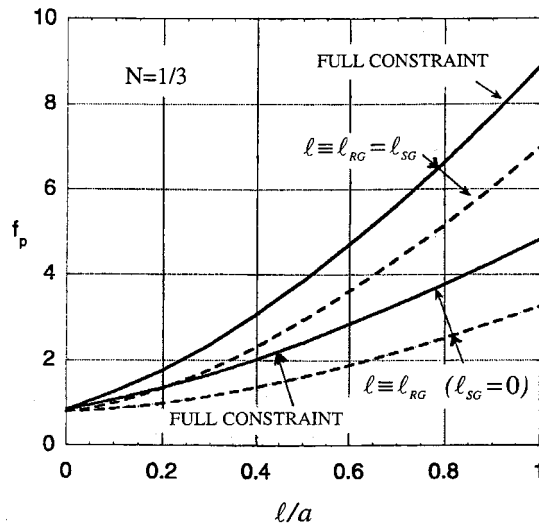
Fig. 5. Effect of higher order boundary conditions on the strengthening factor for a metal matrix composite containing a dilute distribution of spherical particles. Particles of radius a are bonded to a metal matrix characterized by J_2 SGP with constitutive length parameters, (ℓ_{SG}, ℓ_{RG}) (Fleck and Hutchinson, 1997; and unpublished work). The matrix material represented by the lower two curves ($\ell_{SG} = 0$, $\ell \equiv \ell_{RG}$) hardens due to rotation gradients alone and corresponds to the limit of couple stress theory, while the material represented by upper two curves hardens by both stretch and rotation gradients ($\ell \equiv \ell_{SG} = \ell_{RG}$). For each of the two sets of curves, the solid curve corresponds to the imposition of the higher order condition requiring the plastic strains to vanish at the particle/matrix interface. The dashed curve is computed with no constraints on the plastic strains at the interface.

conditions imposed using conventional theory make no distinction between conditions at the free surface of the film and those at the metal/ceramic interface when stressing is in the plane of the film. In fact, according to conventional theory there is no difference under these conditions between the behavior of a detached stretched film and one attached to a substrate. Moreover, conventional theory predicts there is no effect of a very thin passivation layer deposited on top of the free surface. Passivation layers are known to significantly increase the stress changes when the film deforms plastically (Shen et al., 1998). The physical situation at the free surface and the interface are quite different. Dislocations are blocked at the ceramic interface causing pileups such that plastic deformation is highly constrained. By contrast, dislocations are free to pass out of a free surface, and plastic deformation is unimpeded there. A passivation layer restricts dislocation motion at the surface.

The difference in constraints on plastic flow at a free surface and at a metal/ceramic interface can be modeled within the framework of the higher order theory. The results lead to a nonuniform distribution of plastic strain through the thickness of the film. Careful experiments should be able to discern these effects and give a better indication of the necessity of a higher order strain gradient theory of plasticity. Because there are no rotation gradients away from the edges of the film, the length ℓ_{SG} associated with stretch gradients Eq. (7) is the relevant constitutive length parameter in J_2 SGP theory. To test the theory, experiments should be conducted on films of intermediate thickness in the micron range. Very thin films (e.g. tens of nanometers) have relatively few dislocations and these tend to interact simultaneously with the free surface (or passivation layer) and the substrate (Freund, 1990). No continuum plasticity theory is expected to apply in such cases. At the other extreme of thick films (e.g. tens of microns or more), boundary affected regions should comprise only a small fraction of the total thickness, and it would probably be difficult to measure the influence of the free surface or interface on the average stress in the film.

The effect of higher order boundary conditions can be illustrated by an MMC comprised of a dilute, isotropic distribution of rigid spherical particles reinforcing a metal matrix. The particles are equi-sized with a radius a. The metal matrix is described by J_2 SGP theory. Elastic strains are neglected and a tensile stress–strain relation of the power-law form $\sigma/\sigma_0 = (\varepsilon/\varepsilon_0)^N$ is assumed. The overall tensile stress–strain relation of the composite is

$$\frac{\bar{\sigma}}{\sigma_0} = [1 + \rho(1 + N)f_p]\left(\frac{\bar{\varepsilon}}{\varepsilon_0}\right)^N \tag{12}$$

where ρ is the volume fraction of the particles and f_p is the strengthening factor computed from the problem of a single particle in an infinite matrix (Fleck and Hutchinson, 1997). In addition to its dependence on N and the two normalized constitutive length parameters ℓ_{RG}/a and ℓ_{SG}/a, the strengthening factor depends on the conditions prescribed at the particle/matrix interface. Curves of the strengthening factor as a function of the normalized constitute length parameter are shown on Fig. 5 for four cases. In all of the cases, continuity of tractions and displacements are satisfied at the interface. The lower two curves were computed with $\ell_{SG} = 0$ so that only rotation gradients influence the strain gradient hardening. The formulation in these two cases reduces to a couple stress theory which allows for conditions at the rigid particle to be imposed on the normal gradient of tangential displacements ($u_{t,n}$) to the interface. The effect of enforcing u_{tn} to be zero at the interface is reflected by the upper of the lower two curves. For this particular problem, the extra interface conditions are tantamount to requiring the plastic strains at the interface to vanish. The lower curve applies to the case where no constraint is placed on u_{tn} at the interface. Thus, the difference between the lower two curves in Fig. 5 reflects the role of higher order boundary conditions. The comparison between the upper two curves is similar, but now each of the constitutive length parameters has been taken to be nonzero in the computation with $\ell_{SG} = \ell_{RG}$. Both stretch and rotation gradients influence gradient hardening around the particle. In the general case, conditions on the normal derivative of the normal component of displacement to the interface ($u_{n,n}$) can also be prescribed. For the rigid particle bonded to the power law matrix $u_{n,n} = 0$, is a consequence of incompressibility and zero displacements at the interface. The upper most curve in Fig. 5 has been computed with $u_{t,n} = 0$ at the interface, corresponding again to the condition that the plastic strains vanish as the interface is approached. The other curve for this case was computed with no constraint on this normal derivatives, such that plastic strains occur in the metal all the way to the interface. The constraint on plastic flow at the interface increases the strengthening contribution from the particles, but it is not the dominant contribution. The main contribution is due to the strain gradients induced by the particle embedded in the metal matrix.

4. Concluding remarks

As micromechanics continues to be focused on ever finer scales, it is not surprising that theories must be modified to account for new effects. Strong size effects appear in connection with nonuniform plastic deformations at the micron scale. For problems with lengths falling in the range from roughly a fraction of a micron to ten microns, conventional plasticity will completely miss the size-dependence. Moreover at the present time, dislocation mechanics is unable to cope with the complicated interactions among large number of dislocations. Thus the increasingly important micron range falls into the gap between conventional plasticity and dislocation mechanics, motivating strain gradient plasticity theories. Strain gradient theories bring into play new constitutive length parameters. Two distinct length parameters have been identified in the phenomenological J_2 SGP theory, one primarily tied to stretch gradients ($\ell_{SG} \cong 0.25$ to $1\ \mu\mathrm{m}$) and the other to rotation gradients ($\ell_{RG} \cong 5\ \mu\mathrm{m}$).

The array of potential applications for strain gradient plasticity includes many arising in electronics, especially in packaging, and in the micromechanics of structural materials. Conventional plasticity has been employed extensively in micromechanical studies of structural materials (e.g. fracture, void growth, composite yield behavior and composite failure modes such as fiber and particle debonding and pullout). Some of these applications have been within the micron scale and may be suspect. Efforts to link sub-micron fracture processes to macroscopic fracture behavior require an accurate characterization of plasticity at the micron scale because of the strong stress modification brought about by strain gradients. Many applications to 'thick' metal films are apparent, but more work on the theory must first take place to settle issues surrounding the imposition of the boundary conditions at free surfaces and interfaces.

There are a number of open questions in connection with strain gradient plasticity formulations which require resolution. These include the issues of whether a higher order formulation is necessary, and the problem of the most effective way to combine the strains and strain gradients in the phenomenological theory. The situation is not unlike that in the early days of the development of conventional plasticity theory when there was uncertainty about descriptions of yield surfaces and the connection between phenomenological and physical plasticity theories. Elimination of uncertainties in the present formulations will require elucidation from well chosen experiments, physical continuum theories at the single crystal level, and dislocation mechanics.

Acknowledgements

References

Aifantis, E.C., 1984. On the microstructural origin of certain inelastic modes. Trans. ASME J. Eng. Mater. Technol. 106, 326–330.

Aifantis, E.C., 1992. On the role of gradients in the locations of deformation and fracture. Int. J. Eng. Sci. 30 (10), 1279–1299.

Acharya, A., Bassani, J.L., 1996. On non-local flow theories that preserve the classical structure of incremental boundary value problems. In: Pineau, A., Zaoui, A. (Eds.), IUTAM Symp. on Micromechanics of Plasticity and Damage. Kluwer Academic Publishers, pp. 3–10.

Ashby, M.F., 1970. The deformation of plastically non-homogeneous alloys. Philos. Mag. 21, 399–424.

Atkinson, M., 1995. Further analysis of the size effective in indentation hardness tests of some metals. J. Mater. Res. 10, 2908–2915.

Begley, M.R., Hutchinson, J.W., 1998. The mechanics of size-dependent indentation. J. Mech. Phys. Solids 46, 2049–2068.

Cleveringa, H.H.M., van der Giessen, E., Needleman, A., 1997. Comparison of discrete dislocation and continuum plasticity predictions for a composite materials. Acta mater. 45, 3163–3179.

Dai, H., Parks, D.M., 1998. Geometrically-necessary dislocation density in continuum plasticity theory and FEM implementation To be published.

de Borst, R., Muhlhaus, H.B., 1992. Gradient-dependent plasticity: formulation and algorithmic aspects. Int. J. Num. Methods in Engineering 35, 521–539.

De Guzman, M.S., Neubauer, G., Flinn, P., Nix, W.D., 1993. The role of indentation depth on the measured hardness of materials. Mater. Res. Symp. Proc. 308, 613–618.

Drugan, W.J., Willis, J.R., 1996. A micromechanics-based nonlocal constitutive equation and estimates of representative volume element size for elastic composites. J. Mech. Phys. Solids 44, 496–524.

Evans, A.G., Hutchinson, J.W., Wei, Y., 1998. Interface adhesion effects of plasticity and segregation. Acta Mater. to be published.

Fleck, N.A., Muller, G.M., Ashby, M.F., Hutchinson, J.W., 1994. Strain gradient plasticity: theory and experiment. Acta Met. Mater. 42 (2), 475–487.

Fleck, N.A., Hutchinson, J.W., 1994. A phenomenological theory for strain gradient effects in plasticity. J. Mech. Phys. Solids 41, 1825–1857.

Fleck, N.A., Hutchinson, J.W., 1997. Strain gradient plasticity. In: Hutchinson, J.W., Wu, T.T. (Eds.), Adv. in Applied Mechanics, 33, pp. 295–361.

Freund, L.B., 1990. A criterion for arrest of a threading dislocation in a strained epitaxial layer due to an interface misfit dislocation in its path. J. Appl. Phys. 68, 2073–2080.

Gao, H., Huang, Y., Nix, W.D., Hutchinson, J.W., 1999. Mechanism-based strain gradient plasticity-I. Theory. J. Mech. Phys. Solids. 41, 1239–1263.

Huang, Y., Zhang, L., Guo, T.F., Hwang, K.-C., 1997. Mixed mode near-tip fields for cracks in materials with strain-gradient effects. J. Mech. Phys. Solids 45, 439–465.

Lloyd, D.J., 1994. Particle reinforced aluminum and magnesium matrix composites. Int. Mater. Rev. 39, 1–23.

Ma, Q., Clarke, D.R., 1995. Size dependent hardness of silver single crystals. J. Mater. Res. 10, 853–863.

McElhaney, K.W., Vlassak, J.J., Nix, D.W., 1998. Determination of indenter tip geometry and indentation contact area for depth-sensing indentation experiments. J. Mater. Res. 13, 1300–1306.

Mindlin, R.D., 1965. Second gradient of strain and surface tension in linear elasticity. Int. J. Solids Structures 1, 417–438.

Nix, W.D., Gao, H., 1998. Indentation size effects in crystalline materials: A law for strain gradient plasticity. J. Mech. Phys. Solids 46, 411–425.

Poole, W.J., Ashby, M.F., Fleck, N.A., 1996. Micro-hardness of annealed and work-hardened copper polycrystals. Scripta Materialia 34 (4), 559–564.

Shen, Y.-L., Suresh, S., He, M.Y., Bagchi, A., Kienzle, O., Rühle, M., Evans, A.G., 1998. Stress evolution in passivated thin films of Cu on silica. J. Mater. Res. 13, 1928–1937.

Smyshlyaev, V.P., Fleck, N.A., 1996. The role of strain gradients in the grain size effect for polycrystals. J. Mech. Phys. Solids 44 (4), 465–496.

Stelmashenso, M.A., Walls, M.G., Brown, L.M., Miman, Y.V., 1993. Microindentation on W and Mo oriented single crystals: An SEM study. Acta Met. Mater. 41, 2855–2865.

Stölken, J.S., Evans, A.G., 1998. A microbend test method for measuring the plasticity length scale. Acta mater. 46, 5109–5115.

Tadmore, E.B., Miller, R., Phillips, R., Ortiz, M., 1998. J. Mater. Res. to appear.

Toupin, R.A., 1962. Elastic materials with couple stresses. Archive Rational Mechanics Analysis 11, 385–414.

Wei, Y., Hutchinson, J.W., 1997. Steady-state crack growth and work of fracture for solids characterized by strain gradient plasticity. J. Mech. Phys. Solids 45, 1253–1273.

Xia, Z.C., Hutchinson, J.W., 1996. Crack tip fields in strain gradient plasticity. J. Mech. Phys. Solids 44, 1621–1648.